PCCP

Negative ion photodetachment spectroscopy of the Al_3O_2, Al_3O_3, Al_4O_x, Al_5O_x (x = 3–5), Al_6O_5, and Al_7O_5 clusters

Giovanni Meloni, Michael J. Ferguson and Daniel M. Neumark

Department of Chemistry, University of California, Berkeley, CA 94720, USA and Chemical Science Division, Lawrence Berkeley National Laboratory, Berkeley, CA 94720, USA

Received 17th July 2003, Accepted 27th August 2003
First published as an Advance Article on the web 9th September 2003

The Al_3O_2, Al_3O_3, Al_4O_x, Al_5O_x (x = 3–5), Al_6O_5, and Al_7O_5 clusters are studied using negative ion photoelectron spectroscopy. At 266 nm (4.661 eV) laser photodetachment wavelength the spectra of Al_3O_2 and Al_3O_3 present vibrationally resolved features. They show three electronic transitions, due to two different isomers. From Franck–Condon simulations of the Al_3O_2 and Al_3O_3 photoelectron spectra, several vibrational frequencies together with the normal coordinate changes were derived. We obtained approximate electron affinities for Al_3O_2 and Al_3O_3 using the Gaussian 2 model, and calculated isomerization energies for both the anionic and neutral geometries and the experimental adiabatic detachment energies (ADE) of bands X′ and X. The larger aluminum oxide clusters present several structureless bands which likely also result from multiple isomers. The ADEs for the larger clusters increase with size within a cluster series, with the exception of Al_5O_5.

1. Introduction

Amorphous aluminum oxide based catalysts are among the most widely employed solid acid catalysts. They are used in the isomerization of olefins, paraffins, and alkyl aromatics, alkylation of aromatics with alcohols and olefins, and olefins oligomerization and catalytic cracking.[1] They serve as supports or catalytic components for other reactions, such as combustion of methane,[2] denitrogenation of nitrogen-containing heteroaromatic compounds,[3] and dimerization of olefins.[4] The importance of these catalysts has motivated a large number of experimental and theoretical studies to understand the interaction of aluminum with oxygen from a molecular point of view. Recently, the identification of the presence of corundum (Al_2O_3) in stellar grains[5] has stimulated a new interest in aluminum oxide species and how these are formed from the reaction $Al + O_2$. These considerations have motivated a series of experiments in which the photoelectron (PE) spectra of size-selected $Al_xO_y^-$ anions have been measured in order to characterize the structural motifs and trends in the anion and neutral clusters, in particular their dependence on size and stoichiometry. In this paper, we present additional studies of this type, covering $Al_xO_y^-$ clusters with as many as seven aluminum atoms. This study represents the continuation of our investigations to understand the electronic and vibrational structure of group 13 element-containing clusters, such as B_xN_y,[6,7] Al_xP_y,[8] Ga_xP_y,[9] Ga_xAs_y,[10] and In_xP_y.[11,12]

Wang and coworkers[13,14] reported the first PE spectra of aluminum oxide cluster anions, specifically $Al_xO_y^-$ (x = 1–2, y = 1–5) and $Al_3O_y^-$(y = 0–5). These spectra yielded mainly unstructured bands corresponding to transitions between various anion and neutral electronic states, with partially-resolved vibrational structure seen only for $Al_3O_3^-$. Varying the ion source conditions caused the relative intensities of the two lowest energy bands in the PE spectra of $Al_3O_2^-$ and $Al_3O_3^-$ to change considerably, suggesting that these bands originate from different anion isomers. A somewhat higher resolution PE spectrum of $Al_3O_3^-$ was measured by Akin and Jarrold,[15] who also confirmed the presence of multiple isomers of $Al_3O_3^-$ in a hole-burning experiment.[16]

Electronic structure calculations by Ghanty and Davidson,[17] Martinez *et al.*,[18,19] and Cui *et al.*[20] have proved invaluable in interpreting the PE spectra. These calculations showed that Al_3O_2 and Al_3O_3 each have two nearly degenerate isomers with rather different geometries: planar "V" and "kite" structures for Al_3O_2, and kite and "book" structures for Al_3O_3. These structures are shown in Fig. 1.

Density functional theory (DFT) calculations by Ghanty and Davidson[17] find the V isomer to be the ground state for $Al_3O_2^-$ and Al_3O_2, while for Al_3O_3 the energy ordering is reversed in the anion and neutral; the book is the lowest energy structure for $Al_3O_3^-$, while the kite is the ground state for Al_3O_3. The most recent calculation by Martinez *et al.*,[19] a B3LYP/6-311+G(2d,p) DFT calculation with further optimization at the quadratic configuration interaction (QCISD) level, predicts the energy ordering of the isomers to be reversed

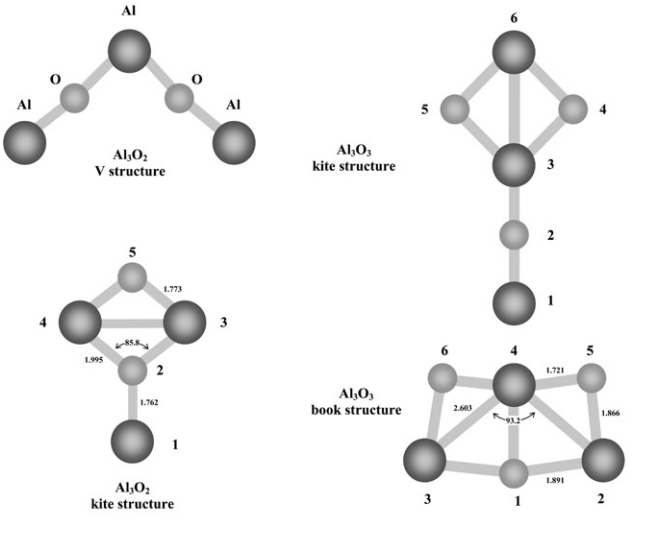

Fig. 1 Structures of the Al_3O_2 and Al_3O_3 clusters optimized at the B3LYP/cc-pVDZ level of theory. The bond lengths, in Å, and angles, in °, are for the $^2A_1$ excited electronic states.

in the anion and neutrals of *both* species. The kite is the global minimum for $Al_3O_2^-$, while the V is the ground state for Al_3O_2, and for Al_3O_3 the orderings are the same as those found by Ghanty and Davidson.[17] These energy reversals are attributed to less positive charge and hence less Coulombic repulsion between the Al atoms in the anions.

For both anions, the calculated energy differences between the two isomers are less than 1 kcal mol^{-1}, with considerably larger splittings ($\sim$10 kcal mol^{-1}) for the neutral isomers. As a result, for each species, both anion isomers should be populated in the PE spectroscopy experiments, and the lowest energy bands in the PE spectra should correspond to transitions between the higher energy anion isomers to the ground state neutral structures (*i.e.* V–V for $Al_3O_2^-$ and kite-kite for $Al_3O_3^-$). In the experimental spectra,[13–16] the relative intensities and the vibrational structure of the lowest energy band for $Al_3O_3^-$ are consistent with the proposed assignments, but a more definitive assignment of the $Al_3O_2^-$ spectrum would be aided by the observation of resolved vibrational structure.

In this paper, we report the first vibrationally resolved PE spectra of $Al_3O_2^-$ at photodetachment energies of 3.493 and 4.661 eV, and somewhat better-resolved PE spectra of $Al_3O_3^-$ than in ref. 16. Electronic structure calculations at the Gaussian 2 (G2) level are carried out in order to refine the energetics of the anion and neutral isomers. Franck–Condon simulations of the vibrational structure in the spectra yield information on the anion and neutral vibrational frequencies and the geometric changes that occur upon photodetachment. We also present the first PE spectra of the $Al_4O_x^-$ and $Al_5O_x^-$ cluster series and of the $Al_6O_5^-$ and $Al_7O_5^-$ clusters, using what we have learned from the smaller clusters to assign some of the features in these spectra.

2. Experiment

The negative ion photoelectron spectrometer used in this investigation has been described in detail previously;[21,22] only a brief description will be given here. $Al_xO_y^-$ anions were produced in a pulsed laser vaporization molecular beam source using argon as carrier gas. A rotating and translating disk of AlN ceramic (>95% dense) or Al is ablated with the second harmonic (2.331 eV, 18 mJ/pulse) of a pulsed Nd:YAG laser. The laser pulses are focused onto the target with a 50 mm lens. The presence of $Al_xO_y^-$ clusters in the molecular beam arises from surface oxidation of the AlN or Al targets. The resulting plasma is entrained in a pulse of Ar carrier gas from a piezoelectric valve. The plasma is expanded through a 19 mm long clustering channel and then passes through a skimmer into a differentially pumped region. Negative ions formed during the expansion are extracted perpendicularly to their flow direction by a pulsed electric field and accelerated to a beam energy of 2.5 keV. The extracted ions enter a linear reflectron time of flight (TOF) mass spectrometer, where they are separated in time and space according to their mass-to-charge ratios. The TOF mass spectrometer resolution is $m/\Delta m \approx 2000$. For this particular experiment the instrument is operated at a repetition rate of 18 Hz.

Mass-selected anions are selectively photodetached with a fixed frequency Q-switched Nd:YAG probe laser. The third (355 nm, 3.493 eV) and fourth (266 nm, 4.661 eV) harmonics were used in this study. The laser is timed so as to photodetach ions of the desired mass. The photoelectron kinetic energy (eKE) is then analyzed by time-of-flight using a 1 m, field-free flight tube. The eKE scale is calibrated using the PE spectra of Cl^-, Br^-, and I^- at 266 nm and O_2^- at 355 nm. The energy resolution is 8–10 meV for an eKE of 0.65 eV and degrades as $(eKE)^{3/2}$ at higher eKE. The PE spectra were taken at two laser polarization angles, 0° and 90° with respect to the direction of electron detection. The laser polarization can be rotated using a half-wave plate.

All photoelectron spectra presented here are plotted as a function of the electron binding energy (eBE) defined as

$$eBE = h\nu - eKE = EA + E^{(0)} - E^{(-)} \quad (1)$$

where $h\nu = 3.493$ and 4.661 eV is the photodetachment energy, EA is the electron affinity of the neutral cluster, and $E^{(0)}$ and $E^{(-)}$ are the internal (electronic + vibrational) energies of the neutral and anion, respectively.

3. Results

3.1 Photoelectron spectra

The 355 and 266 nm PE spectra of $Al_3O_2^-$ and $Al_3O_3^-$ are shown in Fig. 2 and 3, respectively. The 266 nm PE spectra of $Al_4O_x^-$ and $Al_5O_x^-$ (x = 3–5) are presented in Fig. 4 and those of $Al_6O_5^-$ and $Al_7O_5^-$ in Fig. 5. We report only the PE spectra taken at a laser polarization angle of 0° with respect to the flight tube axis; spectra at 90° are similar but lower in intensity. The photoelectron signal is plotted as a function of eBE. At 266 nm, three distinct spectral features are revealed by photodetachment of the $Al_3O_2^-$ and $Al_3O_3^-$ clusters and are labeled X′, X, and A. The 266 nm PE spectra of the larger clusters exhibit several unresolved bands, labeled in alphabetical order.

The 355 nm PE spectrum of $Al_3O_2^-$ shows a weak band, band X′, followed by a much stronger band, band X. Band X′, beginning around 1.5 eV, shows no obvious vibrational structure, but band X shows a partially resolved vibrational progression with a peak spacing of approximately 430 cm^{-1}. The apparent origin of this band is at 2.17 eV. Band A, seen at 266 nm, shows a well-resolved vibrational progression with an apparent origin of 3.40 eV and a frequency of 410 cm^{-1}. Although all three bands were seen previously, no vibrational structure was observed in either band X or A.

All three bands in the PE spectra of $Al_3O_3^-$ show partially-resolved vibrational progressions. The apparent vibrational origin for band X′ is at 2.06 eV, and the spectrum shows a

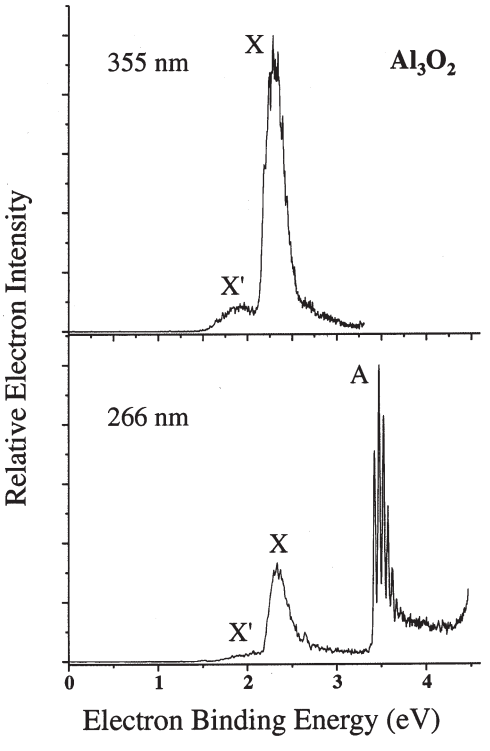

Fig. 2 Photoelectron spectra of $Al_3O_2^-$ at 355 nm (top) and 266 nm (bottom). The laser polarization angle was 0°.

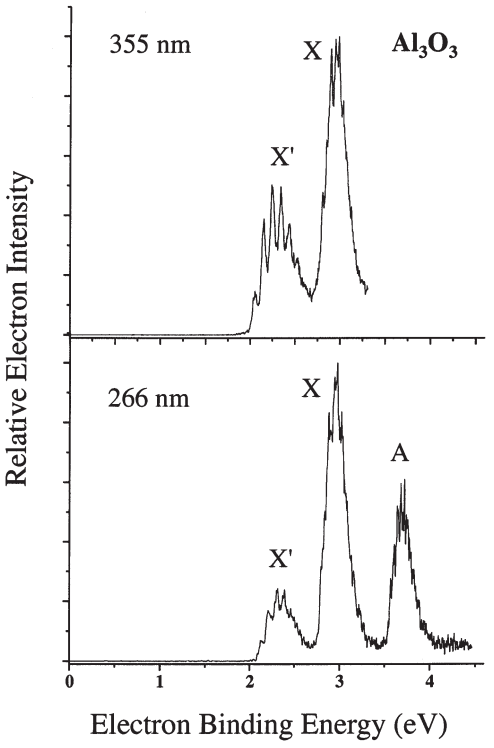

Fig. 3 Photoelectron spectra of $Al_3O_3^-$ at 355 nm (top) and 266 nm (bottom). The laser polarization angle was 0°.

single vibrational progression with a frequency of approximately 770 cm^{-1}. The vibrational structure of band X is more complex; multiple modes appear to be active with partially resolved features spaced by approximately 400 cm^{-1}. Band A exhibits a 300 cm^{-1} progression with its origin at 3.60 eV. Vibrational structure in bands X′ and X was seen previously, but no structure in band A was observed in the earlier work. The X′/X intensity ratio is considerably larger in the $Al_3O_3^-$ spectra than in the $Al_3O_2^-$ spectra.

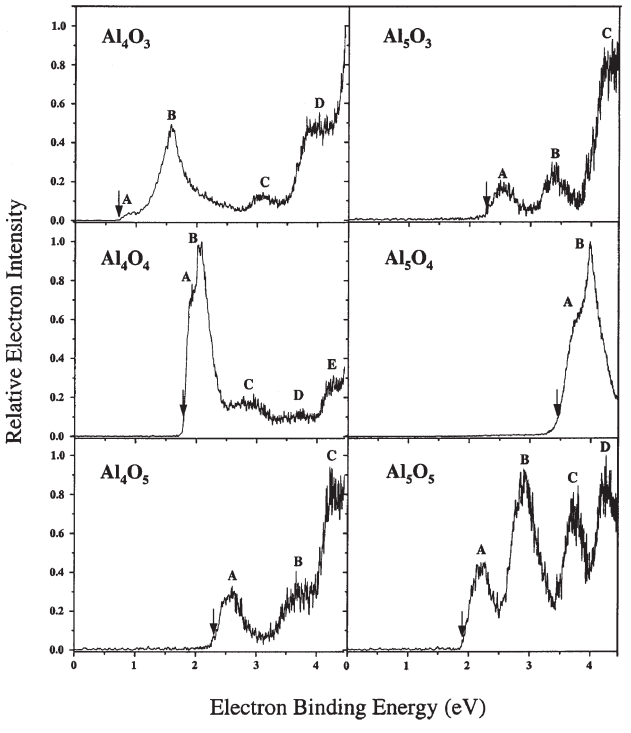

Fig. 4 Photoelectron spectra of $Al_4O_x^-$ and $Al_5O_x^-$ (x = 3– 5) at 266 nm. The laser polarization angle was 0°.

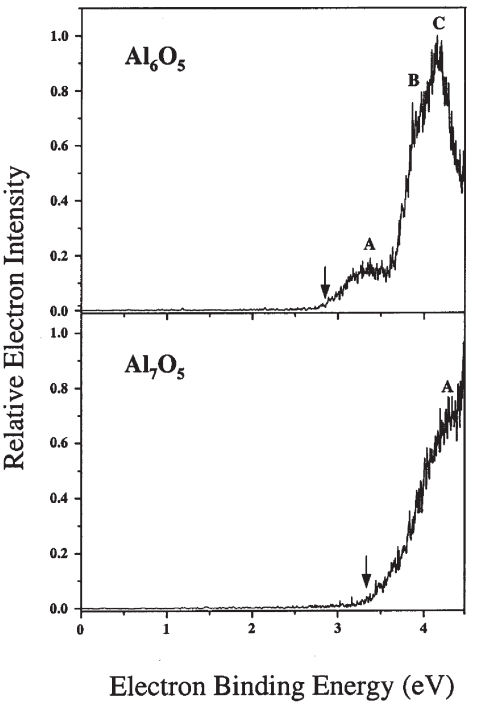

Fig. 5 Photoelectron spectra of $Al_6O_5^-$ and $Al_7O_5^-$ at 266 nm. The laser polarization angle was 0°.

The 266 nm PE spectra of the larger clusters, $Al_4O_x^-$, $Al_5O_x^-$ (x = 3–5), $Al_6O_5^-$, and $Al_7O_5^-$ do not show vibrationally resolved spectral features. Several structureless bands are revealed by photodetachment and labeled in alphabetical order. The vertical detachment energies (VDE) for each band, corresponding to the band maxima, are listed in Table 1, as are the lowest adiabatic detachment energies (ADE), the apparent origins for the lowest energy bands. The ADEs increase within a cluster series with the exception of Al_5O_5, for which band A occurs at lower eBE than the corresponding band for Al_5O_4 and Al_4O_5. The photoelectron spectrum of $Al_7O_5^-$ obtained with 4.661 eV photon energy shows only the onset of band A.

3.2. Electronic structure calculations

To aid in interpretation of the measured PE spectra, we carried out DFT electronic structure calculations on four structural isomers: the V and kite configurations for Al_3O_2 and $Al_3O_2^-$ species, and the kite and book structures for Al_3O_3 and $Al_3O_3^-$. We calculated the optimized geometry, energetics, and vibrational frequencies for the lowest electronic states of each of the anion and neutral isomers, and for the first excited states of the Al_3O_2 kite and Al_3O_3 book isomers.

The computations were performed using the GAUSSIAN98 program suite.[23] The level of theory employed was the DFT

Table 1 Vertical and adiabatic electron detachment energies, in eV, of larger aluminum oxide clusters

Cluster	VEDE	ADE[a]
Al_4O_3	0.94 (A), 1.58 (B), 3.10 (C), 4.09 (D)	0.73(15)
Al_4O_4	1.93 (A), 2.05 (B), 2.83 (C), 3.73 (D), 4.31 (E)	1.78(6)
Al_4O_5	2.59 (A), 3.80 (B), 4.32 (C)	2.30(15)
Al_5O_3	2.56 (A), 3.39 (B), 4.31 (C)	2.20(15)
Al_5O_4	3.83 (A), 3.99 (B)	3.44(10)
Al_5O_5	2.22 (A), 2.91 (B), 3.74 (C), 4.26 (D)	1.89(15)
Al_6O_5	3.40 (A), 4.04 (B), 4.15 (C)	2.82(10)
Al_7O_5	4.35 (A)	3.36(15)

[a] This is the adiabatic detachment energy of band A.

method using the Becke three-parameter exchange functional with the Lee, Yang, and Parr correlation functional (B3LYP). The correlated consistent polarized valence double-ζ basis set (cc-pVDZ) was used for optimizing geometries and vibrational frequencies, and the consistent polarized valence triple-ζ basis set (cc-pVTZ) was used for the energetics of the optimized geometries. We also used the G2 model to perform high accuracy energy calculations on the ground states of the two most stable isomers of $Al_3O_2^-/Al_3O_2$ and $Al_3O_3^-/Al_3O_3$ to gain reliable isomerization energies (ΔE_{isom}). The G2 method is known for its reliability in evaluating thermochemical data[24] of molecules composed of first- and second-row atoms.

Results from the B3LYP and G2 calculations are summarized in Table 2. All calculated structures are planar and have C_{2v} symmetry. The B3LYP geometries calculated for the lowest electronic states of each anion and neutral isomer are essentially identical to those calculated previously by Ghanty and Davidson[17] and Martinez *et al.*,[19] and are not enumerated here. However, the geometries of the first excited states of the Al_3O_2 kite and Al_3O_3 book isomers were not reported previously and are shown in Fig. 1. Molecular orbital (MO) energy diagrams for the two lowest energy structures of $Al_3O_2^-$ and $Al_3O_3^-$ are similar to those reported by Ghanty and Davidson.[17]

The electronic term energy T_e is given for each anion and neutral state; ΔE_{isom} is the energy difference between the electronic and vibrational (assuming harmonic zero-point energy corrections) ground states of the two isomers for each anion and neutral species. For each neutral state, the ADE is listed; this is the energy difference between its vibrational ground state and that of the lowest energy anion isomer.

The results in Table 2 are similar to the previous DFT calculations by Ghanty and Davidson[17] and Martinez *et al.*[18,19] In particular, we find the energetic ordering of the Al_3O_3 isomers to be reversed in the anion and neutral, with kite and book isomers being the lowest energy structures for $Al_3O_3^-$ and Al_3O_3, respectively, just as in the earlier work. However, the energetic ordering of the $Al_3O_2^-$ isomers depends on the method and basis set used. At the B3LYP/aug-cc-pVTZ level of theory,[17] the anion and neutral have the same energetic ordering with the anion V-shape 0.39 kcal mol^{-1} (17 meV) lower in energy than the kite-shape, similar to the results of Ghanty and Davidson.[17] In the B3LYP/cc-pVTZ calculation, this difference is increased to 65 meV. With the smaller cc-pVDZ basis set, the ordering is inverted with the anion kite 83 meV lower in energy than the V, in agreement with the energy ordering found by Martinez *et al.*[19] The G2 calculations, which are expected to yield more accurate energetics, predict the same energy orderings as those found by Martinez *et al.*[19] for the Al_3O_2 and Al_3O_3 anions and neutrals, and predict that the splitting between the two $Al_3O_3^-$ isomers is smaller than that between the two $Al_3O_2^-$ isomers.

4. Discussion

4.1. $Al_3O_2^-$

The electronic structure calculations described in the previous section leave some uncertainty regarding the ground state of $Al_3O_2^-$, and this uncertainty clearly affects the assignment of the experimental PE spectrum. If we assume that the energy orderings in the G2 calculations in Table 2 and ref. 19 are correct, we can assign band X′ of the $Al_3O_2^-$ PE spectrum to the $^2A_1(V) \leftarrow {}^1A_1(V)$ transition, band X to the $^2B_2(kite) \leftarrow {}^1A_1(kite)$ transition, and band A to the $^2A_1(kite) \leftarrow {}^1A_1(kite)$ transition. The lower intensity of band X′ relative to bands X and A reflects the fact that band X′ originates from the slightly higher energy V anion isomer which is expected to be less populated than the kite isomer of $Al_3O_2^-$. If, on the other hand, the V isomer of $Al_3O_2^-$ is the ground state, then we would assign band X′ to the kite ← kite transition originating from the excited anion isomer, and bands X and A to V ← V transitions (the comparable intensities of bands X and A indicate that they both originate from the lowest energy anion isomer). The experimental splitting between bands X and A (~1.2 eV) supports the first assignment, because it is close to the calculated splitting between the ground $^2B_2$ and excited $^2A_1$ states of the neutral kite isomer;[17] the calculated splitting between the ground and excited states of the neutral V isomer is much larger, 3.4 eV.[17]

In order to test our preferred assignment, simulations of bands X′, X, and A were performed within the Franck–Condon (FC) approximation. Using the B3LYP/cc-pVDZ force constants and optimized geometries for the initial state of the anion and the final state of the neutral, we determined the displacement in normal coordinates between the equilibrium structures of various states of $Al_3O_2^-$ and Al_3O_2, $Al_3O_3^-$ and Al_3O_3 within the parallel mode approximation assuming harmonic oscillator potentials. These normal mode displacements and the calculated vibrational frequencies served as the starting point in the simulations and were successively modified to reproduce the experimental PE spectra. Transition origins were taken from experiment and only the most active totally-symmetric modes were considered. The anion vibrational temperature used is 200 K for Al_3O_2 and 300 K for Al_3O_3. The parameters used in the simulations are listed in Table 3. Because some of the vibrational progressions are quite extended, we can obtain vibrational frequencies with higher accuracy than our experimental resolution. The simulated PE spectra are shown in Fig. 6.

Table 2 Results of the electronic structure calculations of $Al_3O_2^-$, Al_3O_2, $Al_3O_3^-$, and Al_3O_3. Adiabatic detachment energies, isomerization energies, and term energies are in eV

			B3LYP[a]			G2		
Species	Structure	State	ADE_e	ΔE_{isom}[b]	T_e	ADE_e	ΔE_{isom}[b]	T_e
$Al_3O_2^-$	Kite-shape	$^1A_1$			0.000			0.000
	V-shape	$^1A_1$		−0.065	−0.056		0.145	0.125
Al_3O_2	V-shape	$^2A_1$	1.393		0.000	1.601		0.000
	Kite-shape	$^2B_2$	1.894	0.562	0.557	2.442	0.605	0.716
	Kite-shape	$^2A_1$	3.026		1.689			
$Al_3O_3^-$	Book-shape	$^1A_1$			0.000			0.000
	Kite-shape	$^1A_1$		0.051	0.046		0.104	0.090
Al_3O_3	Kite-shape	$^2A_1$	1.978		0.000	2.197		0.000
	Book-shape	$^2B_2$	2.518	0.508	0.495	3.044	0.717	0.757
	Book-shape	$^2A_1$	3.182		1.159			

[a] Using cc-pVTZ basis sets. [b] Including zero-point vibrational energy correction.

No vibrational structure is observed for band X′ in the experimental PE spectrum, nor is any seen in the FC simulation of this band, assuming it is the V ← V transition using the calculated normal coordinate displacements and vibrational frequencies. The reason for the absence of structure is seen in Table 3. There are substantial displacements in all four totally symmetric modes. In particular, ΔQ_4 is equal to 0.617 amu$^{1/2}$·Å for the low frequency vibrational mode $\nu_4^{(0)}$ (36 cm^{-1}), corresponding to the symmetric wag of the two terminal Al atoms. These displacements result from the large change in the ∠OAlO bond angle, from 99.8° for $Al_3O_2^-$ to 121.7° for Al_3O_2. As a result, there are overlapping extended progressions in a very low frequency mode, leading to an electronic band in the PE spectrum with no resolved vibrational structure.

At 355 nm, band X exhibits a partially resolved vibrational progression. From the Franck–Condon simulation (see Table 3) we could fit band X using three vibrational active frequencies, in cm^{-1}: 329 ± 50 ($\nu_4^{(0)}$), 430 ± 30 ($\nu_3^{(0)}$), and 780 ± 50 ($\nu_1^{(0)}$). The most active mode is the $\nu_3^{(0)}$ mode, which can be described as the stretching of the two Al atoms in the ring of the kite, Al(3)–Al(4) in Fig. 1. Activity in this mode results from a decrease in the Al(3)–Al(4) bond distance upon photodetachment, from 2.78 to 2.65 Å, according to the electronic structure calculations. The B3LYP computed vibrational frequencies agree well with those obtained in the simulation, and the normal coordinate displacements for the ν_4 and ν_1 modes used to simulate the spectrum are very close to those obtained from the electronic structure calculations. However, the value of ΔQ_3 needed to fit the progression is larger by a factor of 1.8 than the value from the calculated geometries.

The better-resolved vibrational structure in band A can be fit with a FC simulation using frequencies, in cm^{-1}, of 415 ± 30 ($\nu_3^{(0)}$), 663 ± 50 ($\nu_2^{(0)}$), and 768 ± 50 ($\nu_1^{(0)}$), with $\nu_3^{(0)}$ as the main active mode. The computed vibrational frequencies and normal coordinates for both the anion and the neutral are close to those that fit the spectrum, with the exception of ΔQ_3 which needed to be increased by a factor of 2.3 to fit the progression. A weak feature at 3.375 eV assigned as a hot band yields an anion vibrational frequency of $\nu_3^{(-)} = 350 \pm 80$ cm^{-1}.

Both simulations require that ΔQ_3 be increased by about factor of two over the calculated values based on the geometries obtained from the electronic structure calculations. This discrepancy can be reduced by adjusting the geometry of either the anion or both neutral states. The extent of the required geometry change was examined by modifying the geometry of the $^1A_1$ electronic state of $Al_3O_2^-$, keeping fixed the calculated geometries and force constants of the $^2B_2$ and $^2A_1$ states of Al_3O_2. Using a Al(3)–Al(4) bond distance of 3.02 Å, 0.18 Å longer than the optimized calculated value for the $^1A_1$ electronic state of $Al_3O_2^-$, we obtain normal mode displacements ΔQ_3 of 0.514 amu$^{1/2}$ Å for band X and 0.434 amu$^{1/2}$ Å for band A, in better agreement with the best-fit ΔQ_3 values in Table 3.

Overall, we find that all three bands in the $Al_3O_2^-$ PE spectra can be fit with relatively small adjustments to the calculated normal coordinate displacements, assuming the bands are assigned according to the energy ordering of the anion isomers yielded by the G2 calculations. Our analysis therefore confirms this assignment and energy ordering.

The electron affinity (EA) of Al_3O_2 is defined as the energy difference between the v = 0 levels of the anion and neutral electronic ground states, which in this case are the $^1A_1$ kite for $Al_3O_2^-$ and the $^2B_2$ V-structure for Al_3O_2. No transitions between these two different isomers are observed in the PE spectrum. We can, however, determine the EA from the experimental ADE for band X′ and the calculated ΔE_{isom} for the anion isomers, or from the experimental ADE for band X and the calculated ΔE_{isom} for the neutral isomers, according to EA = ADE(X′) + ΔE_{isom} (anion) or EA = ADE(X′) − ΔE_{isom} (neutral). Using the values in Tables 2 and 3, these two determinations yield 1.65 and 1.58 eV, respectively, for the EA's. We select as our best estimate the average of the two values, (1.62 ± 0.12) eV for $EA(Al_3O_2)$. Here the overall error was estimated using the experimental resolution for bands X′ and X together with the uncertainty of the computed value of ΔE_{isom}.

4.2. $Al_3O_3^-$

Based on their own electronic structure calculations and those by Ghanty and Davidson,[17] Akin and Jarrold[15] assigned bands X′ and X in their PE spectrum of $Al_3O_3^-$ to the $^2A_1$(kite) ← $^1A_1$(kite) and $^2B_1$(book) ← $^1A_1$(book) photodetachment transitions. Our electronic structure calculations are consistent with this assignment, and support the new assignment of band A in our spectrum to the $^2B_1$(book) ← $^1A_1$(book) transition. The calculated G2 energetics in Table 2 indicate that the anion

Table 3 Optimized parameters used in the spectral PE simulations within the Franck–Condon approximation. $\nu_i^{(-)}$, in cm^{-1}, is the *i*th vibrational frequency of the anion and $\nu_i^{(0)}$, in cm^{-1}, is the *i*th vibrational frequency of the neutral. The normal mode displacement ΔQ_i is in amu$^{1/2}$ Å. ADEs are in eV and anion temperatures (*T*) in K. The values in parentheses are calculated at the B3LYP/cc-pVDZ level of theory

Species	Band	Structure	State	$\nu^{(-)}$	$\nu^{(0)}$	ΔQ_i	ADE	*T*
Al_3O_2	X′	V-shape	$^2A_1$	ν_4 = 41 (41)	36 (36)	0.617 (0.617)	1.50 ± 0.10	200
				ν_3 = 235 (235)	237 (237)	0.886 (0.886)		
				ν_2 = 436 (436)	444 (444)	1.138 (1.138)		
				ν_1 = 954 (954)	962 (962)	0.045 (0.045)		
	X	Kite-shape	$^2B_2$	ν_4 = 266 (266)	329 (329)	0.047 (0.040)	2.186 ± 0.010	200
				ν_3 = 352 (352)	430 (417)	0.455 (0.258)		
				ν_1 = 833 (833)	780 (780)	0.267 (0.238)		
	A	Kite-shape	$^2A_1$	ν_3 = 352 (352)	415 (391)	0.473 (0.203)	3.419 ± 0.008	200
				ν_2 = 671 (671)	663 (683)	0.077 (0.064)		
				ν_1 = 833 (833)	768 (768)	0.134 (0.104)		
Al_3O_3	X′	Kite-shape	$^2A_1$	ν_4 = 546 (546)	610 (573)	0.320 (0.223)	2.052 ± 0.010	300
				ν_3 = 578 (578)	808 (726)	0.490 (0.447)		
	X	Book-shape	$^2B_2$	ν_5 = 210 (210)	275 (245)	0.385 (0.275)	2.805 ± 0.012	300
				ν_4 = 390 (412)	410 (427)	0.461 (0.329)		
				ν_2 = 610 (664)	690 (623)	0.269 (0.095)		
				ν_1 = 718 (718)	750 (699)	0.085 (0.055)		
	A	Book-shape	$^2A_1$	ν_5 = 210 (210)	283 (256)	0.565 (0.421)	3.610 ± 0.015	300
				ν_4 = 390 (412)	460 (439)	0.255 (0.212)		
				ν_2 = 610 (664)	630 (630)	0.265 (0.201)		

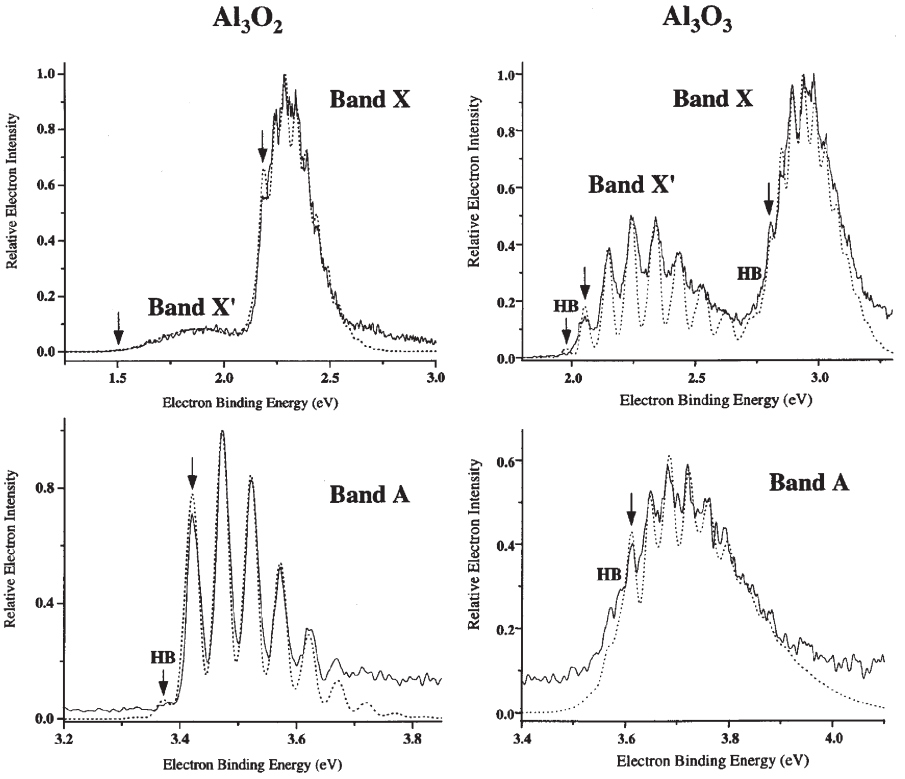

Fig. 6 Spectral simulations (dotted line) within the Franck–Condon approximation superimposed to the experimental PE spectra.

kite isomer is only 0.104 eV higher than book isomer of the anion. Hence, as in the $Al_3O_2^-$ PE spectrum, the lowest energy band does not originate from the anion ground state. However, the X′/X intensity ratio is clearly higher in the $Al_3O_3^-$ PE spectra than in the $Al_3O_2^-$ spectra, even though the ion source conditions were essentially the same when the PE spectra were taken for the two anions. This experimental observation is consistent with the G2 calculations, which show a smaller energy splitting between the two anionic isomers of Al_3O_3 than of Al_3O_2 ($\Delta E_{isom} = 0.145$ eV).

All three bands show resolved vibrational structure. The best-fit FC simulations are shown in Fig. 6, and the parameters used in these simulations are listed in Table 3. Band X′ comprises progressions in the two totally symmetric $\nu_4^{(0)}$ and $\nu_3^{(0)}$ modes with frequencies of 610 and 808 cm^{-1}, respectively, with most of the activity in the $\nu_3^{(0)}$ mode. The ν_4 and ν_3 modes correspond to symmetric stretch and distortion vibrations, respectively, of the kite "head". Activity in these mode results because the Al-O bond lengths in the "head" are longer and more asymmetric in the anion.[17,19] The ADE for this band is found to be (2.052 ± 0.010) eV. The fitting parameters are all quite close to the calculated values, with the most notable difference being that $\nu_3^{(0)}$ frequency used to fit the band is 82 cm^{-1} higher than the calculated frequency.

A similar analysis for band X yields an ADE of (2.805 ± 0.012) eV. The FC simulation involved four vibrational active modes, in cm^{-1}: 275 ± 50 ($\nu_5^{(0)}$), 410 ± 30 ($\nu_4^{(0)}$), 690 ± 50 ($\nu_2^{(0)}$), and 750 ± 50 ($\nu_1^{(0)}$), with $\nu_4^{(0)}$, the symmetric stretching of Al(2) and Al(3) with respect to Al(4), as the main mode. The Al(2)–Al(3) bond distance decreases from 2.52 Å to 2.34 Å upon photodetachment, according to the electronic structure calculations.[17,19] The calculated frequencies agree with the best-fit values, but all of the calculated normal coordinate displacements are somewhat smaller than the best-fit values, indicating that the electronic structure calculations underestimate the geometry change upon photodetachment.

For band A, we find the ADE to be 3.610 eV, yielding a splitting between the neutral $^2A_1$ and $^2B_2$ "book" states of (0.805 ± 0.015) eV. This band was fit assuming three a_1 modes are the most active with the following frequencies, in cm^{-1}: 283 ± 30 ($\nu_5^{(0)}$), 460 ± 50 ($\nu_4^{(0)}$), and 630 ± 50 ($\nu_2^{(0)}$), with $\nu_5^{(0)}$ as the main mode. Two anion frequencies are derived as 210 ± 80 and 390 ± 80 cm^{-1} from the FC simulations; these frequencies yielded the best fit to the spectrum, but do not correspond to isolated transitions and are thus quite uncertain. The agreement for the calculated modes with the best-fit values is good. The normal mode displacement of $\nu_5^{(0)}$ is somewhat larger than the value obtained from the optimized geometries and force constants at the B3LYP/cc-pVDZ level of theory. The ν_5 mode can be described as the bending of the two Al atoms with respect to the central Al(4). The ΔQ_5 underestimation suggests that the calculated $\angle$Al(2)-Al(4)-Al(3) angle change of 4.4° between the anionic ground state and the neutral excited state of Al_3O_3 is too small.

We can extract an approximate EA(Al_3O_3) using the G2 values for ΔE_{isom}(anions) and ΔE_{isom}(neutrals). Following the same approach as for the evaluation of EA(Al_3O_2), we obtained the values of 2.16 and 2.09 eV from the experimental ADE's associated with bands X′ and X, respectively. We select as our best estimate for EA(Al_3O_3) the average of the two values yielding (2.12 ± 0.10) eV. Here the overall error was estimated using the experimental resolution for bands X′ and X together with the uncertainty of the computed value of ΔE_{isom}.

4.3. Larger aluminum oxide clusters

The photoelectron spectra of $Al_4O_x^-$, $Al_5O_x^-$ ($x = 3$–5), $Al_6O_5^-$, and $Al_7O_5^-$ measured at 266 nm represent the first experimental results on these clusters. These spectra do not exhibit resolved vibrational structure. Determination of the VDE's for each band is straightforward, as each corresponds to a band maximum. The ADE of the first band of every spectrum, marked as an arrow in Fig. 4 and 5, is determined from the measured electron binding energy spectrum by extrapolating the linear portion of the first leading edge in the PE spectrum to the energy axis.[25] The crossing between the axis and this line is our best estimate of the ADE. Using this method,

the error bars are 60–150 meV. The adiabatic electron detachment and vertical electron detachment energies are reported in Table 1.

The lowest ADEs increase as the number of Al or O atoms is increased, with the exception of the $Al_5O_5^-$ PE spectrum, which has a lower ADE than the first band of either the $Al_5O_4^-$ or $Al_4O_5^-$ spectrum. Such a result suggests that neutral Al_5O_5 is particularly stable; further insight into why this might the case would be greatly facilitated by electronic structure calculations in this size regime. No *ab initio* or density functional calculations have been performed on these species, except for the neutral Al_4O_4 cluster.[26] The richness in different calculated low-lying energy isomers for the Al_4O_4 cluster is evidenced by five electronic transitions, A–E, observed in the PE spectrum (Fig. 4).

In light of the results for Al_3O_2 and Al_3O_3, contributions from multiple anion isomers are expected in the PE spectra of the larger clusters. The likeliest candidates for such effects are the $Al_4O_3^-$ spectrum, where the weak band A could certainly arise from an anion excited structural isomer, and the $Al_4O_4^-$ and $Al_5O_4^-$ spectra, in which the overlapped bands A and B could originate from transitions from nearly degenerate anion isomers. The computations of Chang *et al.*[26] find that neutral Al_4O_4 has nearly degenerate singlet di-bridged kite (D_{2h}) and triplet cubic isomers 1 (T_d), so these may be the pairs of isomers leading to bands A and B in the $Al_4O_4^-$ PE spectrum. Finally, the appearance of bands A and B in the $Al_5O_3^-$, , $Al_4O_5^-$, and $Al_5O_5^-$ spectra are similar to bands X and X′ in the $Al_3O_3^-$ spectra, so these bands in the larger clusters may also arise from different anion isomers.

The $Al_6O_5^-$ and $Al_7O_5^-$ PE spectra show features at high electron binding energy. Smaller $Al_6O_x^-$ or $Al_7O_x^-$ ($x < 5$) clusters were not observed in the mass spectrum; this together with the high ADE's suggests that $Al_6O_5^-$ and $Al_7O_5^-$ have high stability.

4. Conclusions

The vibrationally resolved photoelectron spectra of $Al_3O_2^-$ and $Al_3O_3^-$ together with PE spectra of larger aluminum oxide clusters have been presented. Three electronic bands in the PE spectra of $Al_3O_2^-$ and $Al_3O_3^-$ are discussed in detail and analyzed with the aid of electronic structure calculations and Franck–Condon simulations of vibrational structure. In the $Al_3O_2^-$ PE spectrum, bands X and A are assigned to a transition originating from the lowest energy "kite" anion isomer, while band X′ originates from the slightly higher energy "V" anion isomer. While these assignments were proposed previously, they are confirmed by the intensities, energetics, and vibrational structure seen in our experimental spectra. Similarly, in the $Al_3O_3^-$ PE spectra, bands X and A originate from the lowest energy "book" anion isomer, while band X′ originates from the slightly higher energy "kite" anion isomer.

Computations using the G2 method showed that ΔE_{isom} for the $Al_3O_3^-$ isomers is lower than ΔE_{isom} for $Al_3O_2^-$, a result consistent with the relative intensities of band X′ and X in the $Al_3O_2^-$ and $Al_3O_3^-$ photoelectron spectra. Using G2 values of ΔE_{isom} for the anions and the neutrals, we could derive the EA(Al_3O_2) of (1.62 ± 0.12) eV and EA(Al_3O_2) of (2.12 ± 0.10) eV.

Although detailed assignments of PE spectra for the larger clusters were not attempted, the general appearance of these spectra also suggests contributions from multiple anion isomers. The results presented here imply that it is worthwhile to investigate the extent of the contribution from multiple isomers to the PE spectra of other semiconductor cluster anions.

Acknowledgements

This research is supported by the National Science Foundation under Grant No. DMR-0139064.

References

1 A. Corma, *Chem. Rev.*, 1995, **95**, 559.
2 A. F. Ahlstromsilversand and C. U. I. Odenbrand, *Appl. Catal. A*, 1997, **153**, 157.
3 S. Rajagopal, T. L. Grimm, D. J. Collins and R. Miranda, *J. Catal.*, 1992, **137**, 453.
4 D. Kiessling, G. Wendt, K. Hagenau and R. Schoellner, *Appl. Catal.*, 1991, **71**, 69.
5 L. R. Nittler, C. M. O. Alexander, X. Gao, R. M. Walker and E. Zinner, *Astrophys. J.*, 1997, **483**, 475.
6 K. R. Asmis, T. R. Taylor and D. M. Neumark, *J. Chem. Phys.*, 1999, **111**, 8838.
7 K. R. Asmis, T. R. Taylor and D. M. Neumark, *J. Chem. Phys.*, 1999, **111**, 10 491.
8 H. Gomez, T. R. Taylor and D. M. Neumark, *J. Phys. Chem. A*, 2001, **105**, 6886.
9 T. R. Taylor, K. R. Asmis, C. S. Xu and D. M. Neumark, *Chem. Phys. Lett.*, 1998, **297**, 133.
10 T. R. Taylor, H. Gomez, K. R. Asmis and D. M. Neumark, *J. Chem. Phys.*, 2001, **115**, 4620.
11 K. R. Asmis, T. R. Taylor and D. M. Neumark, *Chem. Phys. Lett.*, 1999, **308**, 347.
12 H. Gomez, T. R. Taylor, Y. Zhao and D. M. Neumark, *J. Chem. Phys.*, 2002, **117**, 8644.
13 S. R. Desai, H. B. Wu, C. M. Rohlfing and L. S. Wang, *J. Chem. Phys.*, 1997, **106**, 1309.
14 H. B. Wu, X. Li, X. B. Wang, C. F. Ding and L. S. Wang, *J. Chem. Phys.*, 1998, **109**, 449.
15 F. A. Akin and C. C. Jarrold, *J. Chem. Phys.*, 2003, **118**, 5841.
16 F. A. Akin and C. C. Jarrold, *J. Chem. Phys.*, 2003, **118**, 1773.
17 T. K. Ghanty and E. R. Davidson, *J. Phys. Chem. A*, 1999, **103**, 8985.
18 A. Martinez, F. J. Tenorio and J. V. Ortiz, *J. Phys. Chem. A*, 2001, **105**, 8787.
19 A. Martinez, L. E. Sansores, R. Salcedo, F. J. Tenorio and J. V. Ortiz, *J. Phys. Chem. A*, 2002, **106**, 10 630.
20 X. Y. Cui, I. Morrison and J. G. Han, *J. Chem. Phys.*, 2002, **117**, 1077.
21 R. B. Metz, A. Weaver, S. E. Bradforth, T. N. Kitsopoulos and D. M. Neumark, *J. Phys. Chem.*, 1990, **94**, 1377.
22 C. S. Xu, G. R. Burton, T. R. Taylor and D. M. Neumark, *J. Chem. Phys.*, 1997, **107**, 3428.
23 M. J. Frisch, G. W. Trucks, H. B. Schlegel *et al.*, *GAUSSIAN 98 Revision A.9*, Gaussian, Inc., Pittsburgh, PA, 1995.
24 K. Raghavachari, L. A. Curtiss, *Quantum Mechanical Electronic Structure Calculations with Chemical Accuracy*, ed. S. R. Langhoff, Kluwer Academic, Dordrecht, The Netherlands, 1995.
25 C. S. Xu, E. Debeer, D. W. Arnold, C. C. Arnold and D. M. Neumark, *J. Chem. Phys.*, 1994, **101**, 5406.
26 C. Chang, A. B. C. Patzer, E. Sedlmayr, T. Steinke and D. Sulzle, *Chem. Phys. Lett.*, 2000, **324**, 108.